



HAL
open science

Characterization and comparison of groundwater quality and redox conditions in the Arakawa Lowland and Musashino Upland, southern Kanto Plain of the Tokyo Metropolitan area, Japan

Takeshi Saito, Lorenzo Spadini, Hirotaka Saito, Jean Martins, Laurent Oxarango, Takato Takemura, Shoichiro Hamamoto, Per Moldrup, Ken Kawamoto, Toshiko Komatsu

► To cite this version:

Takeshi Saito, Lorenzo Spadini, Hirotaka Saito, Jean Martins, Laurent Oxarango, et al.. Characterization and comparison of groundwater quality and redox conditions in the Arakawa Lowland and Musashino Upland, southern Kanto Plain of the Tokyo Metropolitan area, Japan. *Science of the Total Environment*, 2020, 722, pp.137783. 10.1016/j.scitotenv.2020.137783 . hal-03038834

HAL Id: hal-03038834

<https://hal.science/hal-03038834>

Submitted on 3 Dec 2020

HAL is a multi-disciplinary open access archive for the deposit and dissemination of scientific research documents, whether they are published or not. The documents may come from teaching and research institutions in France or abroad, or from public or private research centers.

L'archive ouverte pluridisciplinaire **HAL**, est destinée au dépôt et à la diffusion de documents scientifiques de niveau recherche, publiés ou non, émanant des établissements d'enseignement et de recherche français ou étrangers, des laboratoires publics ou privés.

1
2
3 **Characterization and comparison of groundwater quality and redox conditions in the Arakawa**
4 **Lowland and Musashino Upland, southern Kanto Plain of the Tokyo Metropolitan area, Japan**
5
6

7 Takeshi Saito¹, Lorenzo Spadini², Hiroataka Saito³, Jean M.F. Martins², Laurent Oxarango², Takato
8 Takemura⁴, Shoichiro Hamamoto⁵, Per Moldrup⁶, Ken Kawamoto¹, and Toshiko Komatsu¹
9

10
11
12 ¹Graduate School of Science and Engineering, Saitama University, Japan
13 255 Shimo-Okubo, Sakura-ku, Saitama 338-8570, JAPAN
14

15 ²Institute of Environmental Geosciences, Grenoble Alps University, France
16 621 Avenue Centrale, 38400 Saint-Martin-d'Hères, FRANCE
17

18 ³Institute of Agriculture, Tokyo University of Agriculture and Technology, Japan
19 3-5-8 Saiwai-cho, Fuchu-shi, Tokyo 183-8509, JAPAN
20

21 ⁴Department of Earth and Environmental Sciences, Nihon University, Japan
22 3-25-40 Sakurajosui, Setagaya-Ku, Tokyo 156-8550, JAPAN
23

24 ⁵Graduate School of Agricultural and Life Sciences, The University of Tokyo, Japan
25 1-1-1, Yayoi, Bunkyo-ku, Tokyo 113-8657, JAPAN
26

27 ⁶Department of Civil Engineering, Aalborg University, Denmark
28 Thomas Manns Vej 23, 1-256, 9220 Aalborg Ø, DENMARK
29
30

31
32 **Corresponding author:**
33

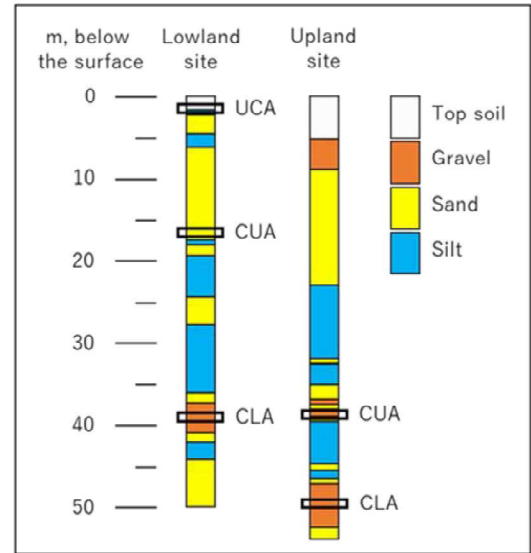
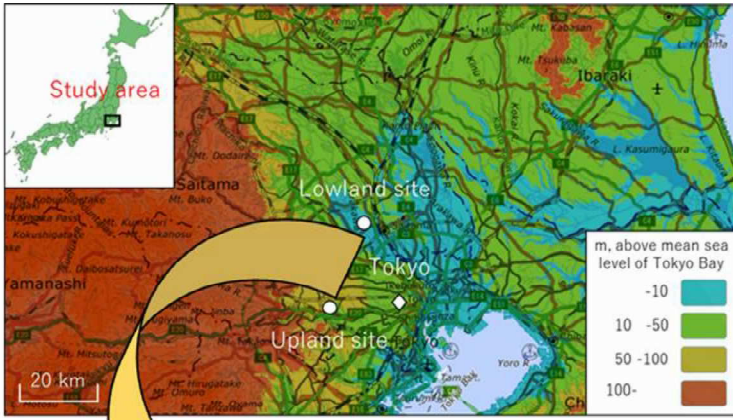
34 Takeshi Saito

35
36 Graduate School of Science and Engineering, Saitama University, Japan
37 255 Shimo-Okubo, Sakura-ku, Saitama, 338-8570, JAPAN
38

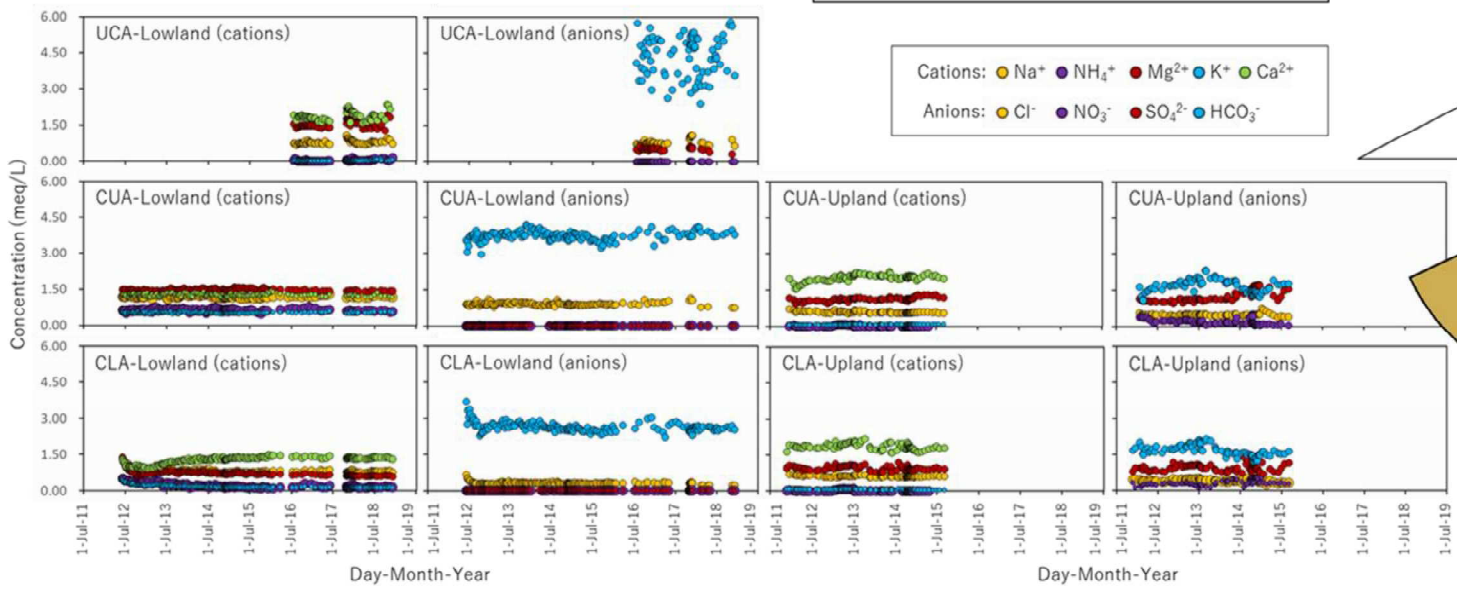
39 TEL: +81-48-858-3572

40 FAX: +81-48-858-7374

41 E-mail: saitou@mail.saitama-u.ac.jp
42
43
44
45
46
47
48
49
50
51
52
53
54
55
56
57
58
59
60
61
62
63
64
65



Long-term groundwater quality



Iron re
conc

Methan
cond

Highlights (3 to 5 bullet points, maximum 85 characters including spaces per bullet point):

Long-term groundwater quality including 35 chemical parameters was monitored.

Five aquifers in the Arakawa Lowland and Musashino Upland of Japan were targeted.

Completely different groundwater redox conditions were observed for both study areas.

Three aquifers in the Lowland were under iron reducing to methanogenic conditions.

Two aquifers in the Upland were under aerobic conditions.

1 **ABSTRACT**

2 Groundwater is essential for the Earth biosphere but is often contaminated by harmful chemical
3 compounds due to both anthropogenic and natural causes. A key factor controlling the fate of
4 harmful chemicals in groundwater is the reduction/oxidation (redox) conditions. The formation
5 factors for the groundwater redox conditions are insufficiently understood. In this study, long-term
6 groundwater quality beneath one of the world megacities was monitored and evaluated. We
7 measured and compared hydrogeochemical conditions including groundwater quality (35 chemical
8 parameters) and redox conditions of five aquifers in the Arakawa Lowland and Musashino Upland,
9 southern Kanto Plain of the Tokyo Metropolitan area, Japan. Monitoring results suggested the
10 following: The main origin of groundwater is precipitation in both the Lowland and Upland areas.
11 The three aquifers in the Arakawa Lowland are likely fully separated, with one unconfined and two
12 confined aquifers under iron reducing and methanogenic conditions, respectively. Oppositely, in the
13 Musashino Upland, the water masses in the two aquifers are likely partly connected, under aerobic
14 conditions, and undergoing the same groundwater recharge and flow processes under similar
15 hydrogeological conditions. The observed very different groundwater redox conditions were likely
16 caused by the difference between groundwater recharge and discharge areas of the Musashino
17 Upland and Arakawa Lowland.

18

19 **Keywords:** Groundwater quality, Groundwater redox conditions, Hydrogeochemical processes,
20 long-term monitoring, Tokyo Metropolitan area of Japan

21

22 **1. Introduction**

23 Fresh water such as river water and groundwater constitute only around 2.5% out of the water on
24 the Earth. The abundance of river water is quite small and is estimated to be approximately 0.006%
25 of freshwater while around 30% of freshwater is groundwater (Shiklomanov, 1998). At least half of
26 the global population depends on groundwater as the source of drinking water (Appelo and Postma,
27 2005). The usage of groundwater is very diverse and includes agricultural, industrial, and drinking
28 water purposes. Around 2.5 billion people depend only on groundwater for their daily water usage
29 (WWAP, 2015). Therefore, groundwater is highly essential for the Earth biosphere from not only
30 qualitative but also quantitative aspects.

31 Groundwater is basically characterized by markedly lower flow rate and longer residence time
32 (approximately 1500 years as a mean value) compared to other fresh water resources including river
33 water which shows an averaged residence time of around 16 days (Shiklomanov, 1998). During the
34 flow processes from recharge area to discharge area, groundwater can be contaminated by harmful
35 chemical compounds due to both anthropogenic and natural factors. One of the most important
36 conditions controlling the fate (solubility, chemical speciation, toxicity, bioavailability, and mobility)

37 of harmful chemical compounds is the reduction/oxidation (redox) conditions in the groundwater.
38 For instance, the fate of arsenic, chromium, inorganic nitrogen (NO_3^- , NO_2^- , and NH_4^+), chlorinated
39 volatile organic compounds (e.g., tetrachloroethene and trichloroethene), and BTEX (benzene,
40 toluene, ethylbenzene, and xylene) is significantly affected by groundwater redox conditions
41 (Blowes et al., 1997; Wiedemeier et al., 1998; Tesoriero et al., 2001; Islam et al., 2004; Aelion et al.,
42 2010; Puckett et al., 2011; Griefßmeier et al., 2017). Groundwater redox conditions are created during
43 microbially induced redox processes. Dissolved oxygen is normally first to be used as electron
44 acceptor. In absence of oxygen, the order of utilization of electron acceptors is generally NO_3^- , Mn
45 (IV), Fe (III), SO_4^{2-} , and CO_2 , resulting in simultaneous production of N_2 , Mn (II), Fe (II), Sulfide
46 (H_2S , HS^- , and S^{2-}), and CH_4 , respectively. Predominant microorganisms significantly change with
47 the progression of these processes and groundwater redox conditions become more reductive
48 (Christensen et al., 2000; Naudet et al., 2004; Appelo and Postma, 2005; McMahon and Chapelle,
49 2007; Tesoriero et al., 2015).

50 In the southern Kanto Plain of the Tokyo Metropolitan area of Japan, groundwater contamination
51 by harmful chemical compounds often occurs due to the extremely high and dense population. To
52 evaluate the fate of harmful chemical compounds and design effective groundwater protection and
53 remediation strategies, fundamental knowledge about groundwater redox conditions and the
54 formation factors for redox conditions in the area is necessary but previous studies regarding

55 groundwater quality in especially the Arakawa Lowland of the southern Kanto Plain are lacking.

56 Further, subsurface warming with temperature increase in the subsurface and groundwater
57 environments has been observed in many areas of the world (Harris and Chapman, 1997; Pollack et
58 al., 1998; Huang et al., 2000; Taniguchi et al., 2003; Perrier et al., 2005; Taniguchi et al., 2007; Kooi,
59 2008). In the Tokyo Metropolitan area as one of megacities in the world, subsurface warming has
60 already been reported by Taniguchi et al. (2007). Subsurface warming, also regarded as subsurface
61 thermal pollution, is caused by surface warming effects such as global warming and urbanization
62 (Huang et al., 2000; Taniguchi et al., 2003). This potentially negative phenomenon may be
63 accelerated by additional and excess exhaust heat from larger underground infrastructures including
64 subways, shopping malls, and sewage systems, especially in the megacities. Subsurface warming can
65 affect physical, chemical, and biological processes in the subsurface and groundwater environments
66 (Banks, 2008; Bonte et al., 2011; Hähnlein et al., 2013) and thereby accelerate changes in
67 groundwater quality. Therefore, the acquisition of long-term monitoring data for groundwater quality
68 as baseline data prior to escalation of subsurface warming is highly essential.

69 The objectives of this study were therefore: (i) to acquire long-term groundwater quality data
70 including 35 chemical parameters for five aquifers in the Arakawa Lowland and Musashino Upland,
71 southern Kanto Plain of the Tokyo Metropolitan area of Japan, representing one of the megacities in
72 the world, (ii) to characterize hydrogeochemistry including the basic interpretation of groundwater

73 quality in each study area based on the acquired long-term monitoring data, and (iii) to compare
74 groundwater redox conditions and discuss the factors creating the difference of redox conditions in
75 both Lowland and Upland areas.

76

77 **2. Materials and methods**

78 **2.1. Site description**

79 The groundwater monitoring sites were established at the campuses of Saitama University
80 (35°51'44.0"N, 139°36'34.0"E) and Tokyo University of Agriculture and Technology (35°41'03.1"N,
81 139°29'07.9"E) in the southern Kanto Plain of the Tokyo Metropolitan area, Japan (Fig. 1a).

82 The Saitama University site is located in the Arakawa Lowland (hereafter, Lowland site) and the
83 altitude at the site is approximately 6.0 m above mean sea level of Tokyo Bay as the reference place
84 in Japan (Fig. 1a). Groundwater monitoring wells were installed in one unconfined (strainer depth:
85 1.5-2.5 m below the surface) and two confined (strainer depths: 15.5-18.4 m below the surface
86 (hereafter, confined upper aquifer) and 37.7-40.0 m below the surface (hereafter, confined lower
87 aquifer)) aquifers (Fig. 1b). A previous study for the stratigraphy and transitions of sedimentary
88 environments in the latest Pleistocene to Holocene sediment core was carried out in very close
89 proximity to the Lowland site (Komatsubara et al., 2010). The unconfined aquifer (Holocene)
90 consists of back marsh deposits with non-marine clayey to silty sediments. In the confined upper

91 aquifer (Holocene), inner bay to delta front deposits are distributed and it consists of silty to sandy
92 marine sediments. The particle size of the sediment in the confined lower aquifer (Pleistocene) is
93 markedly coarser than those of the unconfined and confined upper aquifers and consists of sandy to
94 gravelly fluvial (non-marine) sediments. Further information on the hydrogeological conditions at
95 the Lowland site is presented in Saito et al. (2014); Saito et al. (2016); Brunetti et al. (2017);
96 Ueshima et al. (2017).

97 The Tokyo University of Agriculture and Technology site is located near the border of the
98 Tachikawa Terrace and the Musashino Terrace on the Musashino Upland (hereafter, Upland site) and
99 the altitude at the site is approximately 60 m above mean sea level of Tokyo Bay (Fig. 1a). Two
100 confined (strainer depths: around 38 m below the surface (hereafter, confined upper aquifer) and 50
101 m below the surface (hereafter, confined lower aquifer)) aquifers were targeted in the long-term
102 groundwater quality monitoring (Fig. 1b). Two monitoring wells were installed in each aquifer and
103 are located within several meters distance to each other. Consequently, the acquired data in two wells
104 of each aquifer showed almost the same chemical concentration and characteristics for groundwater
105 quality. Therefore, only the data acquired in one monitoring well of each aquifer is used and
106 discussed in this study. Based on a previous study focusing on analyses of sedimentary facies and
107 depositional environment for sediment cores obtained at the Upland site (Funabiki et al., 2014), both
108 upper and lower aquifers consist of sandy gravels of river channels. Those sediments were formed

109 under non-marine environment during Pleistocene. Additional information of the hydrogeological
110 environments at the Upland site is reported in Saito et al. (2014); Thuyet et al. (2016); Brunetti et al.
111 (2017); Ueshima et al. (2017).

112

113 **2.2. Field works and laboratory analyses**

114 At both monitoring sites, groundwater was periodically sampled from all five aquifers using a
115 sampling bailer (custom-made by ASANO TAISEIKISO ENGINEERING Co., Ltd., Japan) after
116 purging the groundwater of at least two well volumes. The monitoring was started from June 2011 in
117 the confined upper and lower aquifers and July 2016 in the unconfined aquifer at the Lowland site.

118 At the Upland site, monitoring was conducted from November 2011 to October 2015 in both
119 confined upper and lower aquifers. Approximately 160, 180, and 80 samples were obtained in the
120 confined upper and lower aquifers and the unconfined aquifer at the Lowland site, respectively. At
121 the Upland site, approximately 100 samples were taken from each monitoring well in the confined
122 upper and lower aquifers.

123 After groundwater sampling, on-site measurements of water temperature, pH, electric
124 conductivity (EC), dissolved oxygen (DO), and oxidation-reduction potential (ORP) were
125 immediately carried out using portable analyzers (DKK-TOA CORPORATION, Japan) calibrated
126 precisely at each sampling event. The obtained groundwater was immediately filtered using a 0.20

127 μm membrane filter (DISMIC-25CS, Toyo Roshi Kaisha, Ltd., Japan) and chemical analyses
128 described below were carried out in the following days. Major cations (Na^+ , NH_4^+ , K^+ , Mg^{2+} , and
129 Ca^{2+}) and anions (Cl^- , NO_2^- , Br^- , NO_3^- , and SO_4^{2-}), dissolved organic and inorganic carbon (DOC and
130 DIC), and heavy metals and trace elements (Li, B, Al, Si, Cr, Mn, Fe, Ni, Cu, Zn, As, Se, Sr, Cd, Sb,
131 and Pb) were analyzed using an ion chromatograph (HIC-NS, SHIMADZU CORPORATION, Japan
132 or ICS-1500, Nippon Dionex K.K., Japan), TOC analyzer (TOC-V CSH, SHIMADZU
133 CORPORATION, Japan), and ICP-MS (ICPM-8500, SHIMADZU CORPORATION, Japan),
134 respectively. For the DIC, there are three main chemical forms of H_2CO_3 , HCO_3^- , and CO_3^{2-} and
135 their relative abundance ratios are depending on the pH values in water environment (Weathers et al.,
136 2013). In this study, the concentration of HCO_3^- was basically calculated using pH, ionic strength,
137 activity coefficient, and equilibrium constant. For some groundwater samples, semi-quantitative
138 dissolved CH_4 measurements (except for the sample from the unconfined aquifer at the Lowland
139 site) and determination of stable oxygen ($^{18}\text{O}/^{16}\text{O}$) and hydrogen (D (i.e. ^2H)/ ^1H) isotope ratios were
140 conducted using a gas chromatograph (GC-2014, SHIMADZU CORPORATION, Japan) equipped
141 with a thermal conductivity detector (TCD) and a flame ionization detector (FID) and water isotope
142 analyzer (L2130-i, Picarro Inc., USA) based on cavity ring-down spectroscopy, respectively.

143 Another sampling bailer (custom-made by ASANO TAISEIKISO ENGINEERING Co., Ltd.,
144 Japan) allowed for taking out the groundwater without exposure to the air and was used for dissolved

145 CH₄ measurement. Groundwater samples were directly put into analytical vials with approximately
146 60% of the vial volume occupied by the samples. The obtained groundwater in the analytical vials
147 was stored at constant room temperature (20°C) and humidity (60%) for a day to achieve gas-liquid
148 equilibrium inside the vials and was used for measurement of the gas phase in the headspace using a
149 GC-TCD/FID. For stable oxygen and hydrogen isotope ratios, their values are expressed as δ¹⁸O and
150 δD, respectively, which are the relative deviations in per mil (‰, parts per thousand) to Vienna
151 Standard Mean Ocean Water (V-SMOW) as standard solutions. The δ¹⁸O and δD values are given as:

152

$$\delta^{18}O, \delta D = \left(\frac{R_{sample}}{R_{standard}} - 1 \right) \times 1000 (\text{‰}) \quad [1]$$

153

154 where R is the ratio of the heavy to light isotope (¹⁸O/¹⁶O or D/¹H) for groundwater and analytical
155 standards. In addition to the determination of the δ¹⁸O and δD values for some groundwater samples,
156 precipitation was periodically sampled at the Lowland site using a hand-made precipitation collector
157 with anti-evaporation system. The δ¹⁸O and δD values in the precipitation samples were determined
158 based on the same analytical method for revealing the local meteoric water line (discussed below)
159 around the monitoring sites. The precipitation monitoring was carried out every 2 weeks (averaged
160 sampling frequency) from December 2012 to April 2015 and a total of 41 samples were obtained.

161

162 **3. Results and discussion**

163 **3.1. Origin of the groundwater in the Arakawa Lowland and Musashino Upland**

164 Figure 2 illustrates relations between $\delta^{18}\text{O}$ and δD for the precipitation collected at the Lowland
165 site and groundwater in all five aquifers at both Lowland and Upland sites. For the precipitation data
166 monitored from December 2012 to April 2015, the $\delta^{18}\text{O}$ and δD values were markedly variable and
167 ranged from -15.16 to -1.85‰ and -101.38 to -7.32‰, respectively. Linear regression was applied
168 to these plotted data and the obtained equation as the local meteoric water line for the monitoring
169 sites was found to be $\delta\text{D} = 7.19\delta^{18}\text{O} + 7.73$ ($R^2 = 0.93$). A previous study reported the local meteoric
170 water lines in Ogawa town, Utsunomiya city, Kumagaya city, Kashiwa city, and Tsukuba city which
171 are located relatively close to the monitoring sites in this study and all inside the Kanto Plain, Japan.
172 Their local meteoric water lines were found to be $\delta\text{D} = 7.6\delta^{18}\text{O} + 10.3$ ($R^2 = 0.92$), $\delta\text{D} = 8.3\delta^{18}\text{O} +$
173 7.3 ($R^2 = 0.87$), $\delta\text{D} = 7.5\delta^{18}\text{O} + 10.9$ ($R^2 = 0.93$), $\delta\text{D} = 7.4\delta^{18}\text{O} + 8.6$ ($R^2 = 0.98$), and $\delta\text{D} = 7.6\delta^{18}\text{O}$
174 $+ 10.5$ ($R^2 = 0.86$), respectively (Yabusaki et al., 2016). Thus, the equation of the regression line
175 obtained at the Lowland site was quite similar to those of the previous study.

176 Generally, in precipitation formation processes from ocean water evaporation to raindrops
177 formation through condensation, changes in $\delta^{18}\text{O}$ and δD values (i.e. isotopic fractionation) are
178 mainly controlled by the kinetic isotope effect due to different behaviors between lighter isotopes
179 (^1H and ^{16}O) and heavier isotopes (D and ^{18}O). During the evaporation process, lighter isotopes tend

180 to be found in water vapor due to their high vapor pressure, while heavier isotopes are relatively rich
181 in the remaining water. The degree of isotopic fractionation during the evaporation is generally
182 affected by atmospheric humidity and temperature. Oppositely, heavier isotopes tend to be rich in
183 raindrops and the water vapor is simultaneously enriched with lighter isotopes during raindrop
184 formation after condensation. The $\delta^{18}\text{O}$ and δD values in precipitation also change depending on
185 temperature, latitude, altitude, and terrain in the areas where the precipitation occurs (Hoefs, 2004).

186 Craig (1961) found a significant relation between $\delta^{18}\text{O}$ and δD values in 400 samples of water
187 from rivers, lakes, and precipitation as below:

188

$$\delta D = 8\delta^{18}O + 10 \quad [2]$$

189

190 The equation is known as the global meteoric water line and is frequently used in Earth and
191 environmental sciences. Since 1961, the International Atomic Energy Agency (IAEA) has
192 investigated monthly $\delta^{18}\text{O}$ and δD values in precipitation with a global-scale observation network.
193 Based on these long-term monitoring results, Rozanski et al. (1993) gave a global meteoric water
194 line with arithmetic means as below:

195

$$\delta D = (8.17 \pm 0.06)\delta^{18}O + (10.35 \pm 0.65), r^2 = 0.99, n = 206 \quad [3]$$

196

197 The equations of the local meteoric water lines in the Kanto Plain of Japan are similar to the global
198 meteoric water lines, Eqs. [2] and [3].

199 Generally, the $\delta^{18}\text{O}$ and δD values in precipitation vary markedly while in groundwater, they show
200 almost constant values throughout the year due to sufficient mixing of water inside aquifers during
201 infiltration and flowing processes. For the $\delta^{18}\text{O}$ and δD composition in the confined upper and lower
202 aquifers at the Lowland site, more than 40 groundwater samples were analyzed and showed almost
203 constant values compared to those of the precipitation, Fig. 2. In the other three aquifers at the
204 monitoring sites, approximately 20 groundwater samples were measured and the $\delta^{18}\text{O}$ and δD values
205 were also almost constant. The groundwater data from all five aquifers at both Lowland and Upland
206 sites were placed very close to the local meteoric water line around the monitoring sites (Fig. 2). The
207 results suggest that main origin of the groundwater at these study sites is precipitation. We note that
208 the mixing of water with different history such as seawater, fossil water, pore water, formation water,
209 and other water affected by evapotranspiration and/or high degree of reactions with surrounding
210 geology should be considered when $\delta^{18}\text{O}$ and δD values in groundwater are not placed near the local
211 meteoric water line (Hoefs, 2004).

212

213 **3.2. Characterization of hydrogeochemistry in the Arakawa Lowland and Musashino**

214 **Upland**

215 Figure 3 presents temporal variations of major cations and anions (meq/L) in the groundwater
216 from both the unconfined and the confined upper and lower aquifers at the Lowland site and the
217 confined upper and lower aquifers at the Upland site. As mentioned, at least 80 groundwater samples
218 were obtained based on the periodic monitoring and highly valuable long-term and high-resolution
219 groundwater quality data were acquired in each aquifer of the monitoring sites. All five aquifers
220 showed almost constant groundwater quality during the long-term monitoring period over several
221 years. In the unconfined aquifer of the Lowland site, however, the concentration of HCO_3^- was
222 fluctuating and also the electrical balance between the cations and anions within the groundwater
223 was slightly biased toward a negative charge. The electrical balance is given as:

224

$$\text{Electrical Balance (\%)} = \frac{(\text{Sum of cations} + \text{Sum of anions})}{(\text{Sum of cations} - \text{Sum of anions})} \times 100 \quad [4]$$

225

226 where both cations and anions are expressed in concentration unit of meq/L (Appelo and Postma,
227 2005). According to Appelo and Postma (2005), the accuracy of the chemical analysis for major
228 cations and anions in groundwater can be estimated from the calculated electrical balance since the
229 sum of positive and negative charges in groundwater should balance. The electrical balance in the
230 unconfined aquifer at the Lowland site was -14.5% as an averaged value. Also, the mean values of

231 the electrical balance were +4.40%, +4.21%, +3.12%, and +3.15% in the confined upper and lower
232 aquifers at both Lowland and Upland sites, respectively. Because the electrical balance values in all
233 aquifers except for the unconfined aquifer at the Lowland site are less than $\pm 5\%$, the relatively larger
234 averaged value of the electrical balance in the unconfined aquifer at the Lowland site can be
235 explained from the existence of other ionic components and, hence, may be not related to analytical
236 problems. At the beginning of the monitoring in the confined lower aquifer of the Lowland site,
237 decreasing trends for major cations and anions were observed, Fig. 3. This may be associated with
238 the effect of installation of the monitoring wells creating a possibility for the mixing of groundwater
239 from upper aquifers. At the Upland site, the experiment of heated groundwater injection was shortly
240 carried out during 2 months from October to November 2014. The pumped-up groundwater heated
241 to 30°C was continuously injected into the confined lower aquifer at the flow rate of 20 L/min. Even
242 during the experiment period, groundwater quality was almost the same with constant trends
243 compared to the period before starting the experiment. Therefore, to facilitate correct data
244 interpretation, data representing start-up of monitoring in the confined lower aquifer at the Lowland
245 site and during the in-situ thermal experiment at the Upland site are removed for the discussion.

246 All acquired data for major cations and anions in all five aquifers are plotted as a Piper diagram,
247 Fig. 4. A relatively large fluctuating trend was observed for the HCO_3^- concentration in the
248 unconfined aquifer of the Lowland site, Fig. 3. According to Fig. 4, however, the fluctuation seems

249 to be not crucial compared to that of other four aquifers in this study. The averaged chemical
250 concentrations in all five aquifers calculated from the monitoring data in Fig. 4 are shown in Table 1,
251 with standard deviation (1σ). Also, a Schoeller plot and a Stiff diagram were produced based on the
252 mean chemical concentrations (meq/L), Figs. 5 and 6.

253 At the Lowland site, there was almost no NO_3^- with clear SO_4^{2-} detection in the unconfined aquifer,
254 while for the confined upper and lower aquifers, the chemical components of NH_4^+ and CH_4 (Fig. 8)
255 were clearly detected with almost no NO_3^- and SO_4^{2-} present (Figs. 3, 4, 5, and 6 and Table 1). The
256 groundwater in the unconfined and confined lower aquifers consisting of non-marine sediments was
257 a Ca- HCO_3 dominated type (Fig. 6), which is a typical shallow groundwater quality. The confined
258 upper aquifer formed under marine environment showed a completely different trend and was a Na,
259 K, and Mg- HCO_3 dominated type groundwater. Based on these results, all three aquifers indicated
260 significantly different characteristics of water quality, clearly suggesting that these aquifers are
261 completely separate and distinct aquifers. On the other hand, at the Upland site, the chemical
262 components of NO_3^- and SO_4^{2-} were clearly detected with almost no presence of NH_4^+ . Both the
263 confined upper and lower aquifers, which consist of non-marine sediments, showed a Ca- HCO_3
264 dominated type groundwater. All plotted monitoring data for both aquifers in the Piper diagram (Fig.
265 4) clearly overlapped. Further, the figure shapes in the Schoeller plot (Fig. 5) and Stiff diagram (Fig.
266 6) are not significantly different between both aquifers. Thus, the groundwater quality in both

267 aquifers is markedly similar and these aquifers likely represent a unique water circulation system, i.e.
268 the water masses are not fully separated. The groundwater in both aquifers is likely undergoing the
269 same groundwater recharge and flowing processes under very similar hydrogeological conditions
270 such as sedimentary facies and depositional environments.

271

272 **3.3. Comparison of groundwater redox conditions in the Arakawa Lowland and Musashino**

273 **Upland**

274 Figure 7 illustrates a modified Piper diagram for SO_4^{2-} - NH_4^+ - NO_3^- as groundwater redox sensitive
275 chemical species in all five aquifers at both Lowland and Upland sites. Also, a modified Stiff
276 diagram for the averaged concentration of groundwater redox sensitive chemical species plotted
277 using the unit of meq/L (except for CH_4) is shown in Fig. 8. The CH_4 was analyzed based on the
278 semi-quantitative method and the measured data were plotted as % in the headspace gas of analytical
279 vials (see Materials and methods). The Fe concentration was quantified as total dissolved Fe using
280 ICP-MS. Only the chemical form of Fe (II) is possible to be soluble with much less solubility of Fe
281 (III) especially under circumneutral pH conditions. Since the groundwater in all five aquifers showed
282 neutral pH (from 6.5 to 7.6), the concentration of total dissolved Fe is assumed to be nearly equal to
283 Fe (II) concentration. Also, under aerobic groundwater conditions, Fe (II) is generally easy to be
284 oxidized and transformed to the Fe (III) form. Because of the much lower solubility of Fe (III) under

285 neutral range pH conditions, Fe (III)-hydroxides are produced and precipitate under aerobic
286 groundwater conditions (Appelo and Postma, 2005). In the following section, the notation of Fe (II)
287 is therefore used instead of total dissolved Fe.

288 At the Lowland site, a much higher abundance ratio of SO_4^{2-} (more than 90%) was observed (Fig.
289 7) with a very low abundance ratio of NH_4^+ and almost no NO_3^- presence in the unconfined aquifer.
290 Relatively high concentration of Fe (II) was detected (Fig. 8), up to around 10 mg/L. The
291 concomitant presence of these three redox sensitive species (NH_4^+ , Fe (II), and SO_4^{2-}) with almost no
292 NO_3^- existence suggests that the groundwater was under intermediate anaerobic and iron reducing
293 condition. The groundwater from the confined upper and lower aquifers is characterized by the high
294 NH_4^+ abundance ratio > 90%, almost no NO_3^- and SO_4^{2-} existence, and a clear CH_4 detection (0.7%
295 and 1.6% as mean values in the upper and lower aquifers, respectively). Because of the evidence for
296 both almost no SO_4^{2-} detection (instead of sulfide) and CH_4 detection, the groundwater is suggested
297 to be under strong (complete) anaerobic and methanogenic conditions. Sometimes (not
298 systematically analyzed), the concentration of sulfide was measured at low concentration levels in
299 both aquifers, based on the simple and semi-quantitative colorimetric method. The sulfide
300 concentration was slightly higher in the confined upper aquifer than that in the confined lower
301 aquifer. Almost no SO_4^{2-} detection indicates complete sulfate (SO_4^{2-}) reduction to sulfide (H_2S and
302 HS^-). Sulfide is well known to be a strongly complexing transition metal and one of the most

303 common metal complexes found is iron sulfide and the hereby formed insoluble minerals (e.g. Pyrite,
304 Marcasite, Mackinawite, and Troilite). The groundwater in both aquifers is suggested to be under
305 methanogenic (strong anaerobic) condition with less sulfide (H_2S and HS^-) and Fe (II)
306 (approximately 35 $\mu\text{g/L}$ and 60 $\mu\text{g/L}$ as average in the confined upper and lower aquifers,
307 respectively). Hence, the dissolved iron and sulfide aqueous concentrations may be limited from
308 mineral iron sulfide precipitation in these aquifers.

309 The groundwater in the confined upper and lower aquifers at the Upland site showed completely
310 different trends, especially for the behaviors of redox sensitive species compared to the results at the
311 Lowland site. The combined abundance ratios of NO_3^- and SO_4^{2-} reached more than 90% with a very
312 low abundance ratio of NH_4^+ (Fig. 7). Also, there was no CH_4 (under the detection limit), Fig. 8.
313 These results suggest that the groundwater in both aquifers is under aerobic condition with much
314 lower Fe (II) concentration in the groundwater, approximately 25 $\mu\text{g/L}$ as a mean value.

315 Groundwater redox conditions were highly different at the Upland and Lowland sites. Generally,
316 groundwater redox conditions are controlled by several hydrogeochemical and microbial factors,
317 including the mineral composition, the concentration of redox sensitive species, and the type and
318 activity of microorganisms. Also, the difference of groundwater flow systems such as groundwater
319 recharge area or discharge area can affect the formation of groundwater redox conditions (Gascoyne,
320 1997; Gómez et al., 2006). The groundwater in recharge areas may be under aerobic conditions due

321 to less progress of microbially induced redox processes with relatively short groundwater residence
322 time, while for groundwater in discharge areas, there is a possibility of the existence of anaerobic
323 conditions. At the Lowland site, the monitoring site is located in the Arakawa Lowland and the area
324 is generally considered as a groundwater discharge area in terms of broad groundwater flow systems
325 due to markedly low altitude only several meters above sea level, Fig. 1a. The groundwater in the
326 unconfined and the two confined aquifers was probably under iron reducing and methanogenic
327 conditions, respectively, because microbially induced redox processes were likely evolved
328 sufficiently during groundwater flow.

329 At the Upland site, the monitoring site is located in the Musashino Upland and the groundwater in
330 confined aquifers is likely recharged by the precipitation, river water, and the unconfined aquifer in
331 the Upland area (Sindou, 1968). Therefore, the Upland site may be located relatively close to the
332 groundwater recharge areas compared to the Lowland site and thus aerobic groundwater conditions
333 in two confined aquifers are maintained at the Upland site. Further investigation on mineral
334 composition and type and activity of microorganisms is needed for sufficiently clarifying formation
335 factors of these completely different groundwater redox conditions at both sites.

336

337 **4. Conclusions**

338 Long-term groundwater quality including 35 chemical parameters for five aquifers in the Arakawa

339 Lowland and Musashino Upland, southern Kanto Plain of the Tokyo Metropolitan area of Japan,
340 representing one of the megacities in the world was monitored. Based on these data,
341 hydrogeochemistry including groundwater quality and redox conditions was characterized and
342 compared for both Lowland and Upland areas. The factors creating the difference of groundwater
343 redox conditions were discussed.

344 The monitoring of stable oxygen and hydrogen isotope ratios for groundwater in five aquifers as
345 well as precipitation in the Arakawa Lowland suggested that the main origin of groundwater is the
346 precipitation in both Lowland and Upland areas. The acquired long-term and high-resolution
347 groundwater quality data with at least 80 groundwater samples obtained in each aquifer showed
348 almost constant groundwater quality during the monitoring period over several years. According to
349 the acquired data, the three aquifers in the Arakawa Lowland are likely completely separate and
350 distinct aquifers, while the two aquifers in the Musashino Upland, are not fully separated and the
351 groundwater in the two aquifers are undergoing the same groundwater recharge and flow processes
352 under very similar hydrogeological conditions.

353 The behavior of the groundwater redox sensitive chemical species revealed that an unconfined
354 aquifer in the Arakawa Lowland was probably under intermediate anaerobic and iron reducing
355 conditions. Strong anaerobic and methanogenic conditions were found in other two confined
356 aquifers in the Arakawa Lowland. Oppositely, in the Musashino Upland, the groundwater in two

357 confined aquifers was found to be under aerobic conditions. The completely different groundwater
358 redox conditions are suggested due to the difference of groundwater flow systems including the
359 groundwater recharge and discharge areas. The degree of progress in microbially induced redox
360 processes evolved with groundwater flow was likely different in the Upland and Lowland areas with
361 the processes markedly more pronounced in the Arakawa Lowland.

362 Current research status on relationships between groundwater flow systems including recharge
363 area or discharge area and groundwater redox conditions is still insufficient and more research is
364 needed based on long-term and comprehensive investigation of groundwater quality and redox
365 conditions in different parts of the world and, also, representing other megacities.

366

367 **Acknowledgments**

368 This study was supported by Core Research for Evolutionary Science and Technology (CREST)
369 by Japan Science and Technology Agency (JST), a Grant-in Aid for Scientific Research (no.
370 26889015 and 16K20954) and Bilateral Joint Research Projects with the National Center for
371 Scientific Research (CNRS) in France by the Japan Society for the Promotion of Science (JSPS), and
372 Research Grants by LIXIL JS Foundation (no. 15-63) and The Iwatani Naoji Foundation, Japan. The
373 determination of stable oxygen and hydrogen isotope ratios in precipitation and groundwater
374 samples was conducted by the support of Joint Research Grant for the Environmental Isotope Study

375 of Research Institute for Humanity and Nature (RIHN), Japan. The authors deeply appreciate
376 Professor Emeritus Takanori Nakano, Professor Ichiro Tayasu, Dr. Ki-Cheol Shin, and Dr. Shiho
377 Yabusaki all of RIHN for supporting the stable isotope analysis.

378

379 **References**

380 Aelion, C.M., Höhener, P., Hunkeler, D., Aravena, R., 2010. Environmental Isotopes in
381 Biodegradation and Bioremediation. CRC Press, Boca Raton, USA.

382 Appelo, C.A.J., Postma, D., 2005. Geochemistry, Groundwater and Pollution, 2nd Edition. A.A.
383 Balkema Publishers, Leiden, the Netherlands.

384 Banks, D., 2008. An Introduction to Thermogeology: Ground Source Heating and Cooling.
385 Blackwell Publishing Ltd., Oxford, UK. <https://doi.org/10.1002/9781118447512>

386 Blows, D.W., Ptacek, C.J., Jambor, J.L., 1997. In-situ remediation of Cr (IV)-contaminated
387 groundwater using permeable reactive walls: Laboratory studies. Environmental Science &
388 Technology 31 (12), 3348-3357. <https://doi.org/10.1021/es960844b>

389 Bonte, M., Stuyfzand, P.J., Hulsmann, A., van Beelen, P., 2011. Underground thermal energy
390 storage: Environmental risks and policy developments in the Netherlands and European Union.
391 Ecology and Society 16 (1), 22.

392 Brunetti, G., Saito, H., Saito, T., Šimůnek, J., 2017. A computationally efficient pseudo-3D model

393 for the numerical analysis of borehole heat exchangers. *Applied Energy* 208, 1113-1127.
394 <https://doi.org/10.1016/j.apenergy.2017.09.042>

395 Christensen, T.H., Bjerg, P.L., Banwart, S.A., Jakobsen, R., Heron, G., Albrechtsen, H.J., 2000.
396 Characterization of redox conditions in groundwater contaminant plumes. *Journal of Contaminant*
397 *Hydrology* 45 (3-4), 165-241. [https://doi.org/10.1016/S0169-7722\(00\)00109-1](https://doi.org/10.1016/S0169-7722(00)00109-1)

398 Craig, H., 1961. Isotopic variations in meteoric waters. *Science* 133, 1702-1703.
399 <https://doi.org/10.1126/science.133.3465.1702>

400 Funabiki, A., Naya, T., Saito, H., Takemura, T., 2014. Sedimentary facies and depositional
401 environment of CRE-TAT-1 and CRE-TAT-2 drilling core in Fuchu-city, Tokyo, central Japan.
402 *Journal of the Sedimentological Society of Japan*. 73 (2), 137-152 (in Japanese with English
403 abstract). <https://doi.org/10.4096/jssj.73.137>

404 Gascoyne, M., 1997. Evolution of redox conditions and groundwater composition in
405 recharge-discharge environments on the Canadian Shield. *Hydrogeology Journal* 5 (3), 4-18.
406 <https://doi.org/10.1007/s100400050253>

407 Gómez, P., Turrero, M.J., Garralón, A., Peña, J., Buil, B., Cruz, B. de la, Sánchez, M., Sánchez, D.M.,
408 Quejido, A., Bajos, C., Sánchez, L., 2006. Hydrogeochemical characteristics of deep
409 groundwaters of the Hesperian Massif (Spain). *Journal of Iberian Geology* 32 (1), 113-131.

410 Griebmeier, V., Bremges, A., McHardy, A.C., Gescher, J., 2017. Investigation of different nitrogen

411 reduction routes and their key microbial players in wood chip-driven denitrification beds.
412 Scientific Reports 7, 17028. <https://doi.org/10.1038/s41598-017-17312-2>

413 Hähnlein, S., Bayer, P., Ferguson, G., Blum, P., 2013. Sustainability and policy for the thermal use of
414 shallow geothermal energy. Energy Policy 59, 914-925.
415 <https://doi.org/10.1016/j.enpol.2013.04.040>

416 Harris, R.N., Chapman, D.S., 1997. Borehole temperatures and a baseline for 20th-century global
417 warming estimates. Science 275, 1618-1621. <https://doi.org/10.1126/science.275.5306.1618>

418 Hoefs, J., 2004. Stable Isotope Geochemistry. Springer-Verlag, Berlin Heidelberg, Germany.
419 <https://doi.org/10.1007/978-3-662-05406-2>

420 Huang, S., Pollack, H.N., Shen, P.-Y., 2000. Temperature trends over the past five centuries
421 reconstructed from borehole temperatures. Nature 403, 756-758. <https://doi.org/10.1038/35001556>

422 Islam, F.S., Gault, A.G., Boothman, C., Polyá, D.A., Charnock, J.M., Chatterjee, D., Lloyd, J.R.,
423 2004. Role of metal-reducing bacteria in arsenic release from Bengal delta sediments. Nature 430,
424 68-71. <https://doi.org/10.1038/nature02638>

425 Komatsubara, J., Kimura, K., Fukuoka, S., Ishihara, Y., 2010. Sedimentary facies and physical
426 properties of the latest Pleistocene to Holocene sediment core (GS-SSS-1) in the Arakawa
427 Lowland, Saitama City, central Japan. Journal of the Sedimentological Society of Japan 69 (1),
428 3-15 (in Japanese with English abstract). <https://doi.org/10.4096/jssj.69.3>

429 Kooi, H., 2008. Spatial variability in subsurface warming over the last three decades; Insight from
430 repeated borehole temperature measurements in The Netherlands. *Earth and Planetary Science*
431 *Letters* 270 (1-2), 86-94. <https://doi.org/10.1016/j.epsl.2008.03.015>

432 McMahon, P.B., Chapelle, F.H., 2008. Redox processes and water quality of selected principal
433 aquifer systems. *Ground Water* 46 (2), 259-271. <https://doi.org/10.1111/j.1745-6584.2007.00385.x>

434 Naudet, V., Revil, A., Rizzo, E., Bottero, J.-Y., Bégassat, P., 2004. Groundwater redox conditions
435 and conductivity in a contaminant plume from geoelectrical investigations. *Hydrology and Earth*
436 *System Sciences* 8 (1), 8-22. <https://doi.org/10.5194/hess-8-8-2004>

437 Perrier, F., Le Mouel, J.-L., Poirier, J.-P., Shnirman, M.G., 2005. Long-term climate change and
438 surface versus underground temperature measurement in Paris. *International Journal of*
439 *Climatology* 25 (12), 1619-1631. <https://doi.org/10.1002/joc.1211>

440 Pollack, H.N., Huang, S., Shen, P.-Y., 1998. Climate change record in subsurface temperatures: A
441 global perspective. *Science* 282, 279-281. <https://doi.org/10.1126/science.282.5387.279>

442 Puckett, L.J., Tesoriero, A.J., Dubrovsky, N.M., Nitrogen contamination of surficial aquifers - A
443 growing legacy. *Environmental Science & Technology* 45 (3), 839-844.
444 <https://doi.org/10.1021/es1038358>

445 Rozanski, K., Araguás-Araguás, L., Gonfiantini, R., 1993. Isotopic patterns in modern global
446 precipitation. In: *Climate change in continental isotopic records. Geophysical Monograph* 78, 1-36.

447 <https://doi.org/10.1029/GM078p0001>

448 Saito, T., Hamamoto, S., Mon, E.E., Takemura, T., Saito, H., Komatsu, T., Moldrup, P., 2014.

449 Thermal properties of boring core samples from the Kanto area, Japan: Development of predictive

450 models for thermal conductivity and diffusivity. *Soils and Foundations* 54 (2), 116-125.

451 <https://doi.org/10.1016/j.sandf.2014.02.004>

452 Saito, T., Hamamoto, S., Ueki, T., Ohkubo, S., Moldrup, P., Kawamoto, K., Komatsu, T., 2016.

453 Temperature change affected groundwater quality in a confined marine aquifer during long-term

454 heating and cooling. *Water Research* 94, 120-127. <https://doi.org/10.1016/j.watres.2016.01.043>

455 Shiklomanov, I.A., 1998. *World Water Resources: A New Appraisal and Assessment for the 21st*

456 *Century*. UNESCO International Hydrological Programme (IHP), Paris, France.

457 Shindou, S., 1968. Hydrogeology of the Musashino Terrace. *Journal of Geography* 77 (4), 223-246

458 (in Japanese with English Abstract). https://doi.org/10.5026/jgeography.77.4_223

459 Taniguchi, M., Shimada, J., Uemura, T., 2003. Transient effects of surface temperature and

460 groundwater flow on subsurface temperature in Kumamoto Plain, Japan. *Physics and Chemistry*

461 *of the Earth A/B/C* 28 (9-11), 477-486. [https://doi.org/10.1016/S1474-7065\(03\)00067-6](https://doi.org/10.1016/S1474-7065(03)00067-6)

462 Taniguchi, M., Uemura, T., Jago-on, K., 2007. Combined effects of urbanization and global warming

463 on subsurface temperature in four Asian cities. *Vadose Zone Journal* 6 (3), 591-596.

464 <https://doi.org/10.2136/vzj2006.0094>

465 Tesoriero, A.J., Löffler, F.E., Liebscher, H., 2001. Fate of origin of 1,2-Dichloropropane in an
466 unconfined shallow aquifer. *Environmental Science & Technology* 35 (3), 455-461.
467 <https://doi.org/10.1021/es001289n>

468 Tesoriero, A.J., Terziotti, S., Abrams, D.B., 2015. Predicting redox conditions in groundwater at a
469 regional scale. *Environmental Science & Technology* 49 (16), 9657-9664.
470 <https://doi.org/10.1021/acs.est.5b01869>

471 Thuyet, D.Q., Saito, H., Saito, T., Moritani, S., Kohgo, Y., Komatsu, T., 2016. Multivariate analysis
472 of trace elements in shallow groundwater in Fuchu in western Tokyo Metropolis, Japan.
473 *Environmental Earth Sciences* 75: 559. <https://doi.org/10.1007/s12665-015-5170-4>

474 Ueshima, M., Takemura, T., Saito, T., Ito, Y., Hamamoto, S., Saito, H., Komatsu, T., 2017.
475 Relationship between trace elements and depositional environments in shallow sediments: A case
476 study from Southern Kanto Plain, Central Japan. *Environmental Earth Sciences* 76: 633.
477 <https://doi.org/10.1007/s12665-017-6968-z>

478 Weathers, K.C., Strayer, D.L., Likens, G.E., 2013. *Fundamentals of Ecosystem Science*. Academic
479 Press, New York, USA. <https://doi.org/10.1016/C2009-0-03622-8>

480 Wiedemeier, T.H., Swanson, M.A., Moutoux, D.E., Gordon, E.K., Wilson, J.T., Wilson, B.H.,
481 Kampbell, D.H., Haas, P.E., Miller, R.N., Hansen, J.E., Chapelle, F.H., 1998. Technical Protocol
482 for Evaluating Natural Attenuation of Chlorinated Solvents in Ground Water. United States

483 Environmental Protection Agency, Cincinnati, USA.

484 WWAP (United Nations World Water Assessment Programme), 2015. The United Nations World
485 Water Development Report 2015: Water for a Sustainable World. UNESCO, Paris, France.

486 Yabusaki, S., Shimano, Y., Suzuki, Y., 2016. Characteristics of stable isotopes in precipitation at
487 Kanto district, Fukushima City, Matsumoto City and Kyoto City-Variation of stable isotopes in
488 precipitation due to climate change and prediction of its future-. Journal of Japanese Association
489 of Hydrological Sciences 46 (2), 139-155 (in Japanese with English Abstract).
490 <https://doi.org/10.4145/jahs.46.139>

Table[Click here to download Table: Table \(final\).docx](#)

Table 1 Averaged concentration of major cations (Na^+ , NH_4^+ , Mg^{2+} , K^+ , and Ca^{2+}) and anions (Cl^- , NO_3^- , SO_4^{2-} , and HCO_3^-) (meq/L) in the groundwater from three aquifers (UCA, CUA, and CLA) at the Lowland site and two aquifers (CUA and CLA) at the Upland site. UCA, CUA, and CLA stand for unconfined aquifer, confined upper aquifer, and confined lower aquifer, respectively. Values in parentheses express standard deviation (1σ).

Component	Concentration unit	UCA-Lowland		CUA-Lowland		CLA-Lowland		CUA-Upland		CLA-Upland	
Na^+	mg/L	18.07	(1.89)	27.93	(1.44)	18.88	(1.48)	13.85	(0.90)	14.30	(1.21)
NH_4^+	mg/L	0.59	(0.63)	11.54	(0.95)	3.56	(1.43)	0.36	(0.57)	0.40	(0.63)
K^+	mg/L	1.24	(0.67)	19.84	(0.93)	5.65	(1.46)	3.42	(0.39)	2.42	(0.61)
Mg^{2+}	mg/L	18.69	(1.76)	17.71	(0.62)	8.34	(0.78)	13.74	(0.93)	11.67	(1.17)
Ca^{2+}	mg/L	37.83	(3.63)	25.29	(1.01)	25.41	(2.72)	40.53	(3.09)	37.58	(2.65)
Cl^-	mg/L	28.52	(4.54)	32.37	(2.35)	10.71	(1.08)	17.03	(1.16)	14.40	(1.70)
NO_3^-	mg/L	0.26	(0.31)	0.12	(0.25)	0.18	(0.28)	13.12	(5.29)	16.65	(4.96)
SO_4^{2-}	mg/L	24.95	(2.94)	0.23	(0.41)	0.05	(0.13)	56.15	(6.52)	44.96	(6.21)
HCO_3^-	mg/L	265.80	(51.30)	228.16	(12.09)	159.57	(8.57)	108.73	(14.64)	104.90	(11.73)

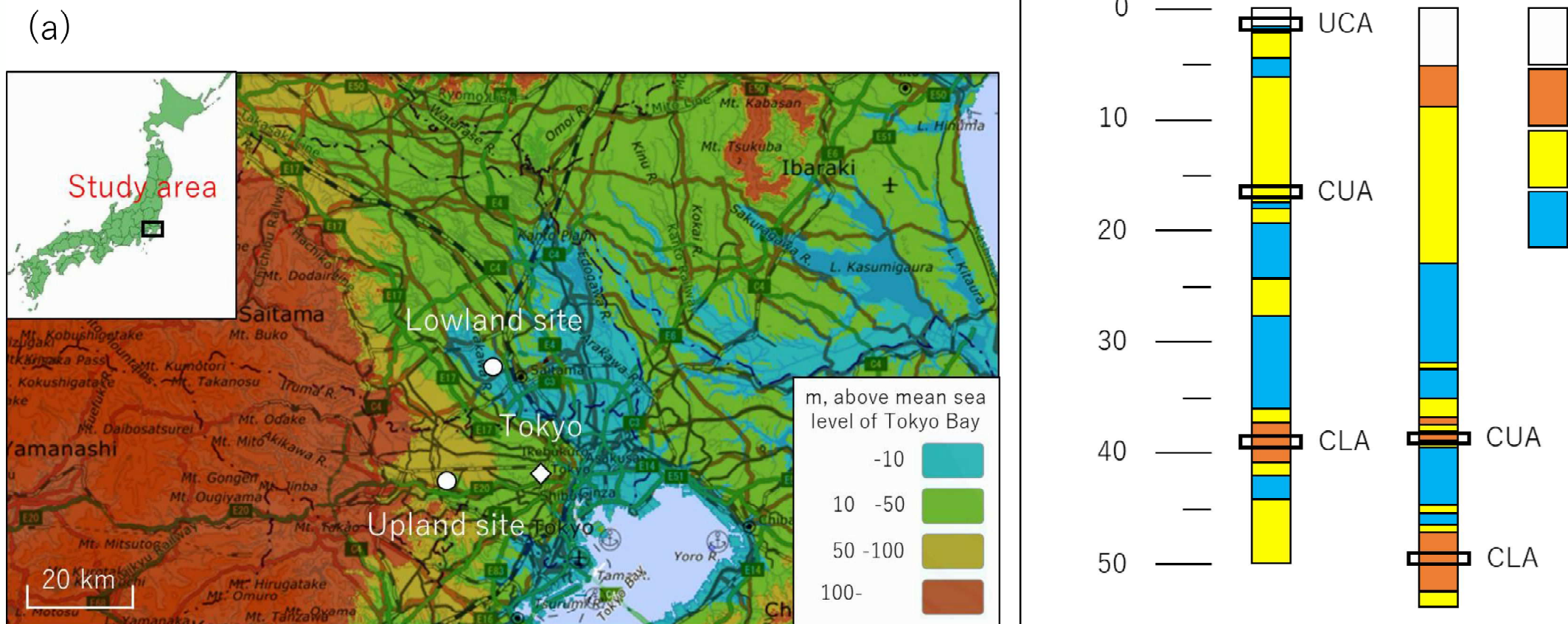


Fig. 1 (a) Location of established groundwater monitoring sites at the campuses of Saitama University and Tokyo University of Agriculture and Technology in the Arakawa Lowland (Lowland site) and Musashino Upland (Upland site), respectively, in the southern Kanto Plain of the Tokyo Metropolitan area of Japan (the base map was taken from Geospatial Information Authority of Japan), and (b) geological columns with monitored three aquifers (UCA, CUA, and CLA) at the Lowland site and two aquifers (CUA and CLA) at the Upland site. UCA, CUA, and CLA stand for unconfined aquifer, confined upper aquifer, and confined lower aquifer, respectively.

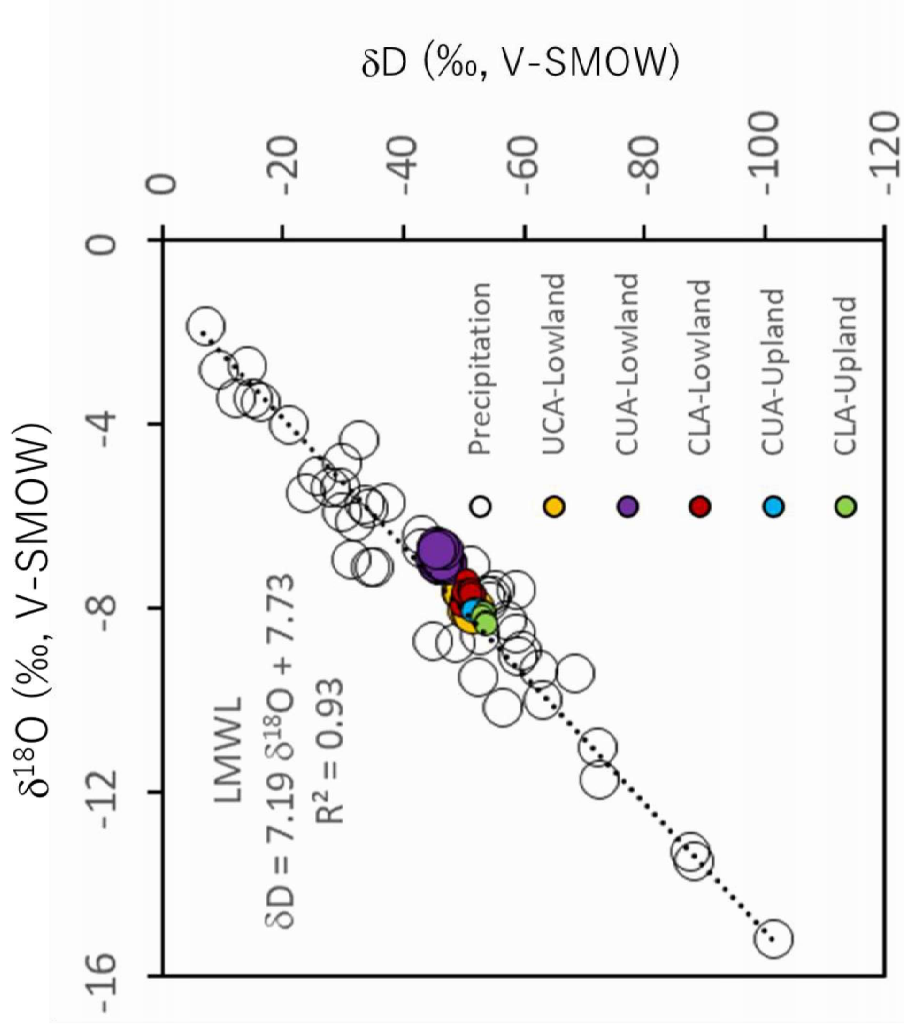


Fig. 2 Relationships between $\delta^{18}\text{O}$ and δD (‰, V-SMOW) for the precipitation at the Lowland site, and the ground water at the Upland site, and the ground water at the Lowland site, and the ground water at the Upland site. LMWL stands for local meteoric water line, unconfined aquifer, and confined upper aquifer, and confined lower aquifer, respectively.

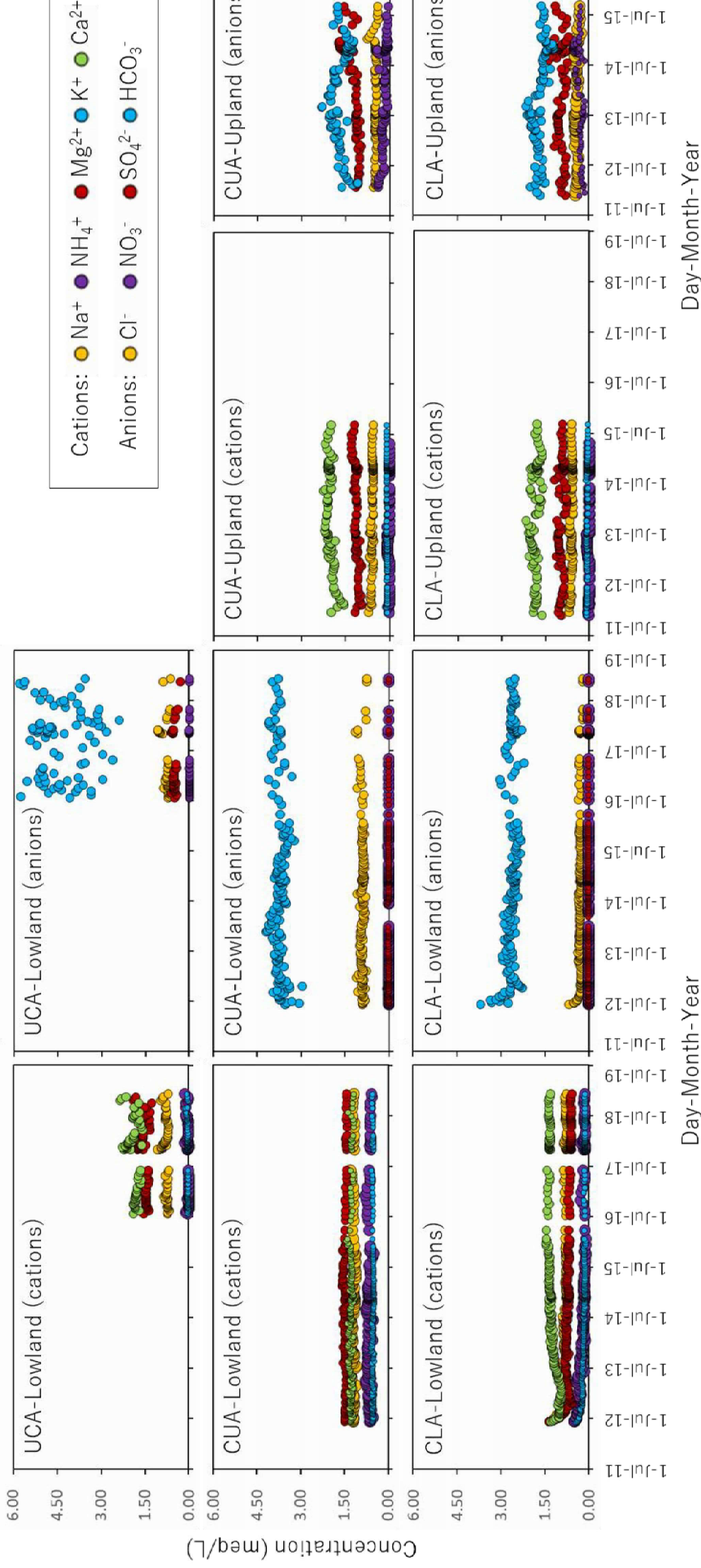


Fig. 3 Temporal variations of the concentration of major cations (Na^+ , NH_4^+ , Mg^{2+} , K^+ , and Ca^{2+}) and anions (Cl^- and HCO_3^-) (meq/L) in the groundwater from three aquifers (UCA, CUA, and CLA) at the Lowland site and two aquifers (UCA, CUA, and CLA) at the Upland site. UCA, CUA, and CLA stand for unconfined aquifer, confined upper aquifer, and confined lower aquifer, respectively.

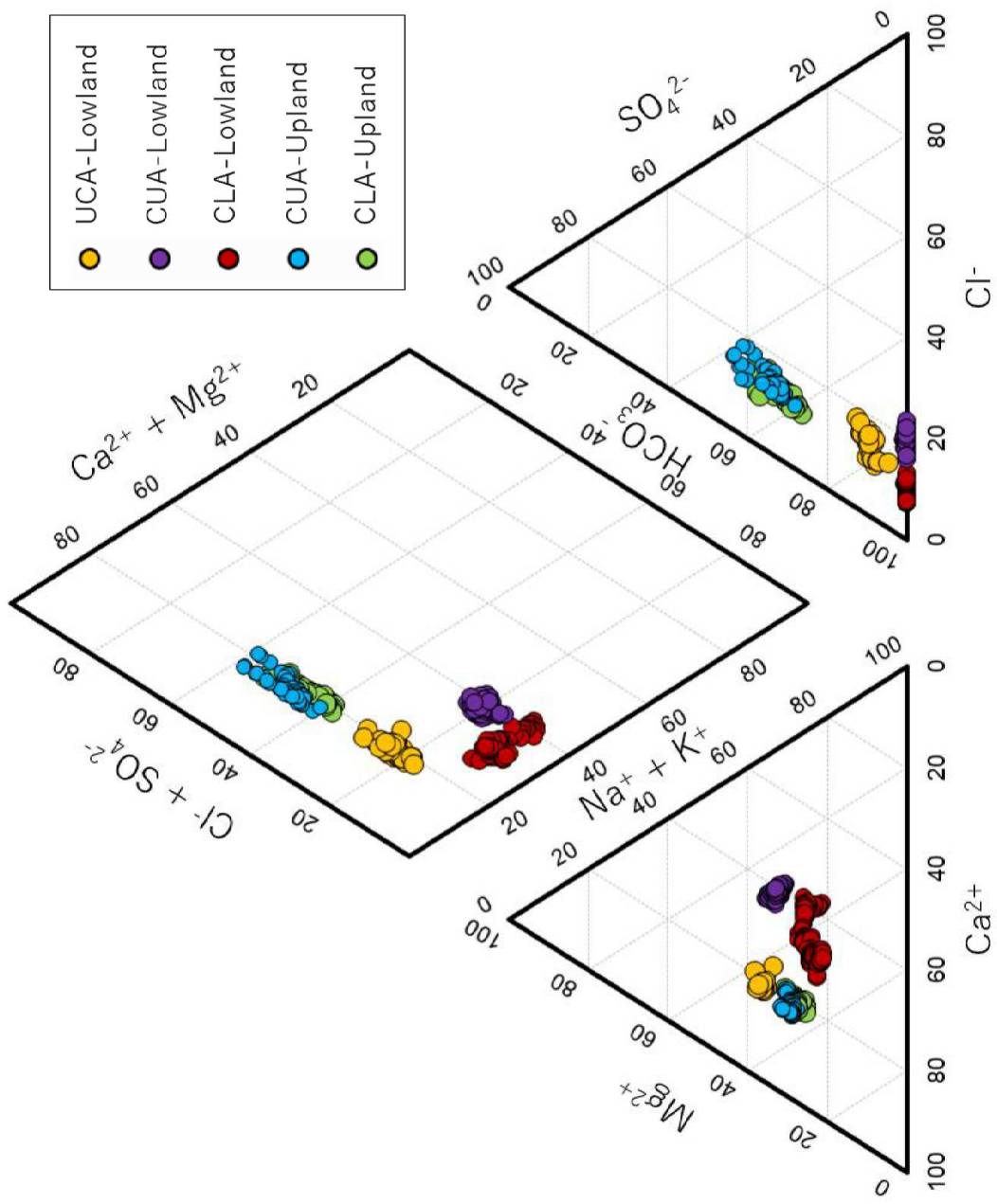


Fig. 4 A Piper diagram for the groundwater from three aquifers (UCA, CUA, and CLA) at the Lowland site and two (CUA and CLA) at the Upland site. UCA, CUA, and CLA stand for unconfined aquifer, confined upper aquifer, and lower aquifer, respectively.

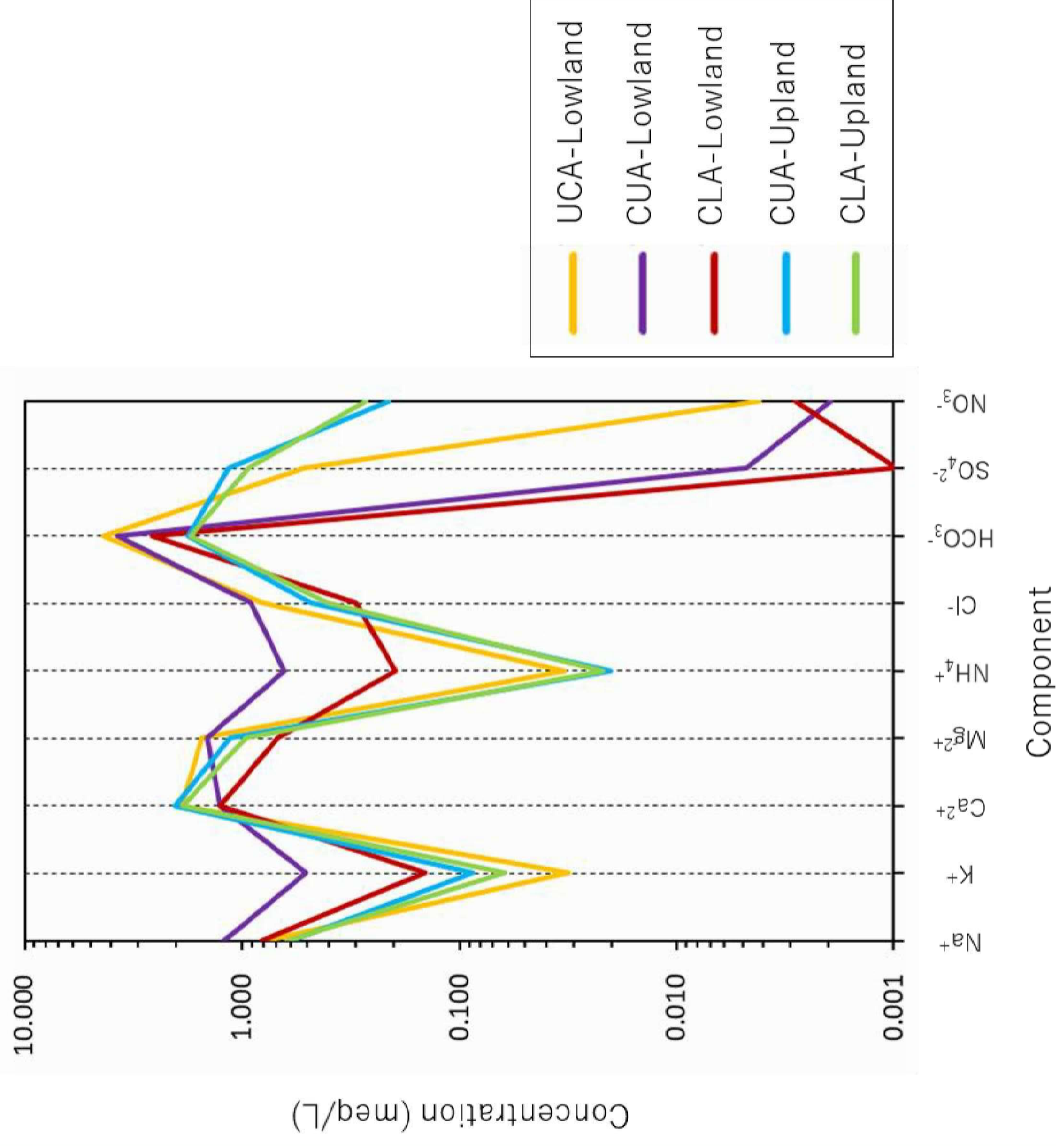


Fig. 5 A Schoeller plot for averaged concentration of major cations (Na^+ , NH_4^+ , Mg^{2+} , K^+ , and Ca^{2+}) and anions (SO_4^{2-} , and HCO_3^-) (meq/L) in the groundwater from three aquifers (UCA, CUA, and CLA) at the Lowland site and (CUA and CLA) at the Upland site. UCA, CUA, and CLA stand for unconfined aquifer, confined upper aquifer, and lower aquifer, respectively.

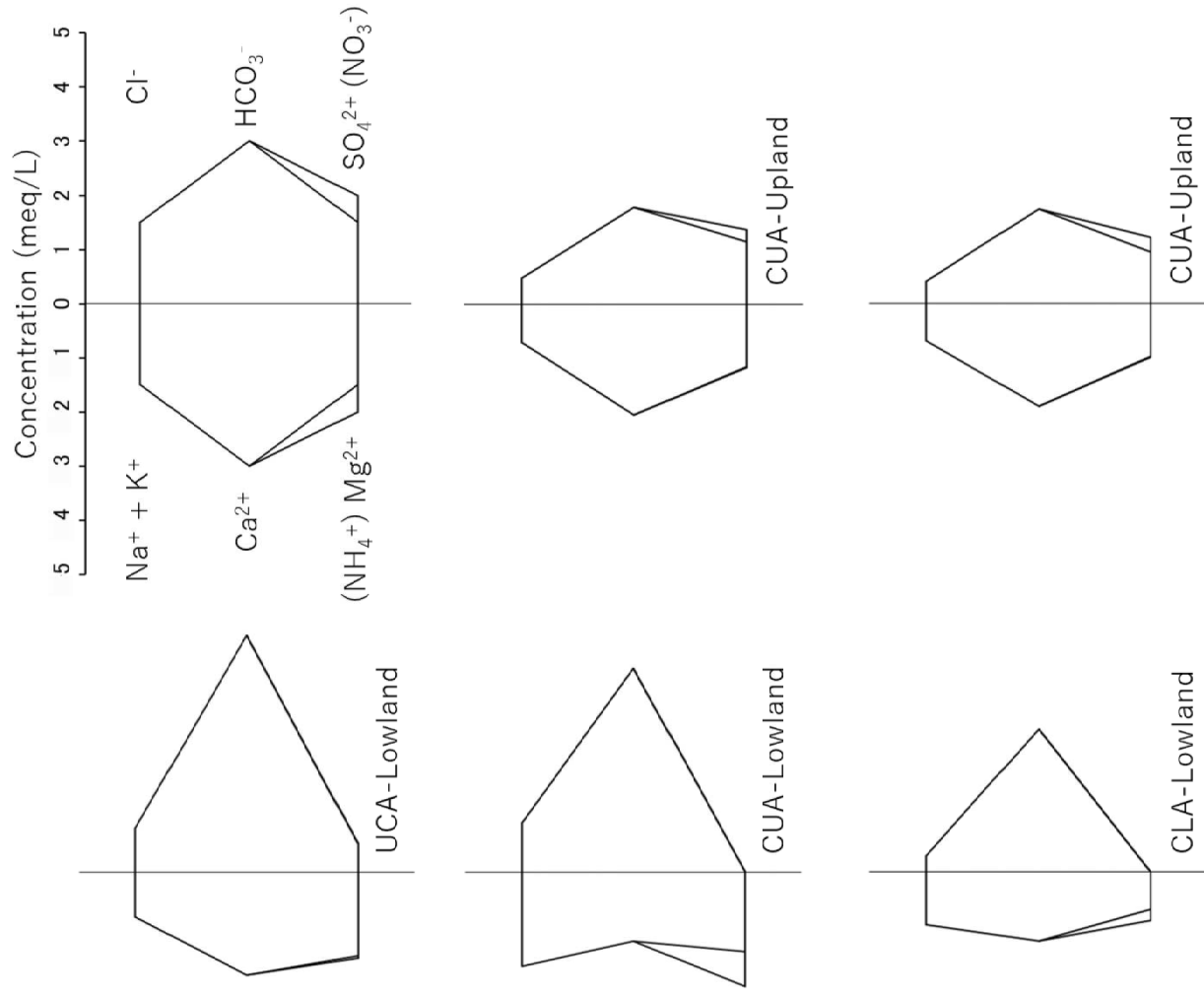


Fig. 6 A Stiff diagram for averaged concentration of major cations (Na⁺, NH₄⁺, Mg²⁺, K⁺, and Ca²⁺) and anions (Cl⁻ and HCO₃⁻) (meq/L) in the groundwater from three aquifers (UCA, CUA, and CLA) at the Lowland site and two aquifers (UCA and CLA) at the Upland site. UCA, CUA, and CLA stand for unconfined aquifer, confined upper aquifer, and confined lower aquifer, respectively.

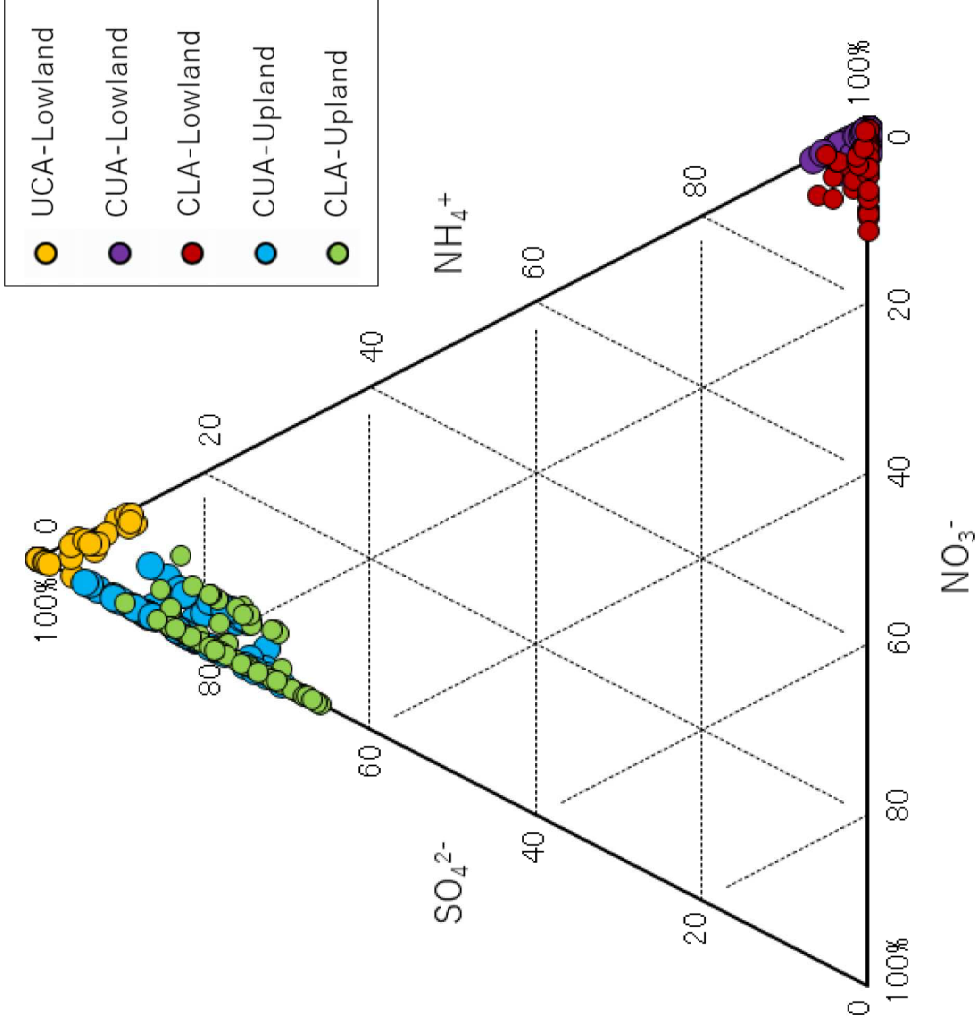


Fig. 7 A modified Piper diagram for SO_4^{2-} , NH_4^+ , and NO_3^- as groundwater redox sensitive chemical species in the groundwater from three aquifers (UCA, CUA, and CLA) at the Lowland site and two aquifers (CUA and CLA) at the site. UCA, CUA, and CLA stand for unconfined aquifer, confined upper aquifer, and confined lower aquifer, respectively.

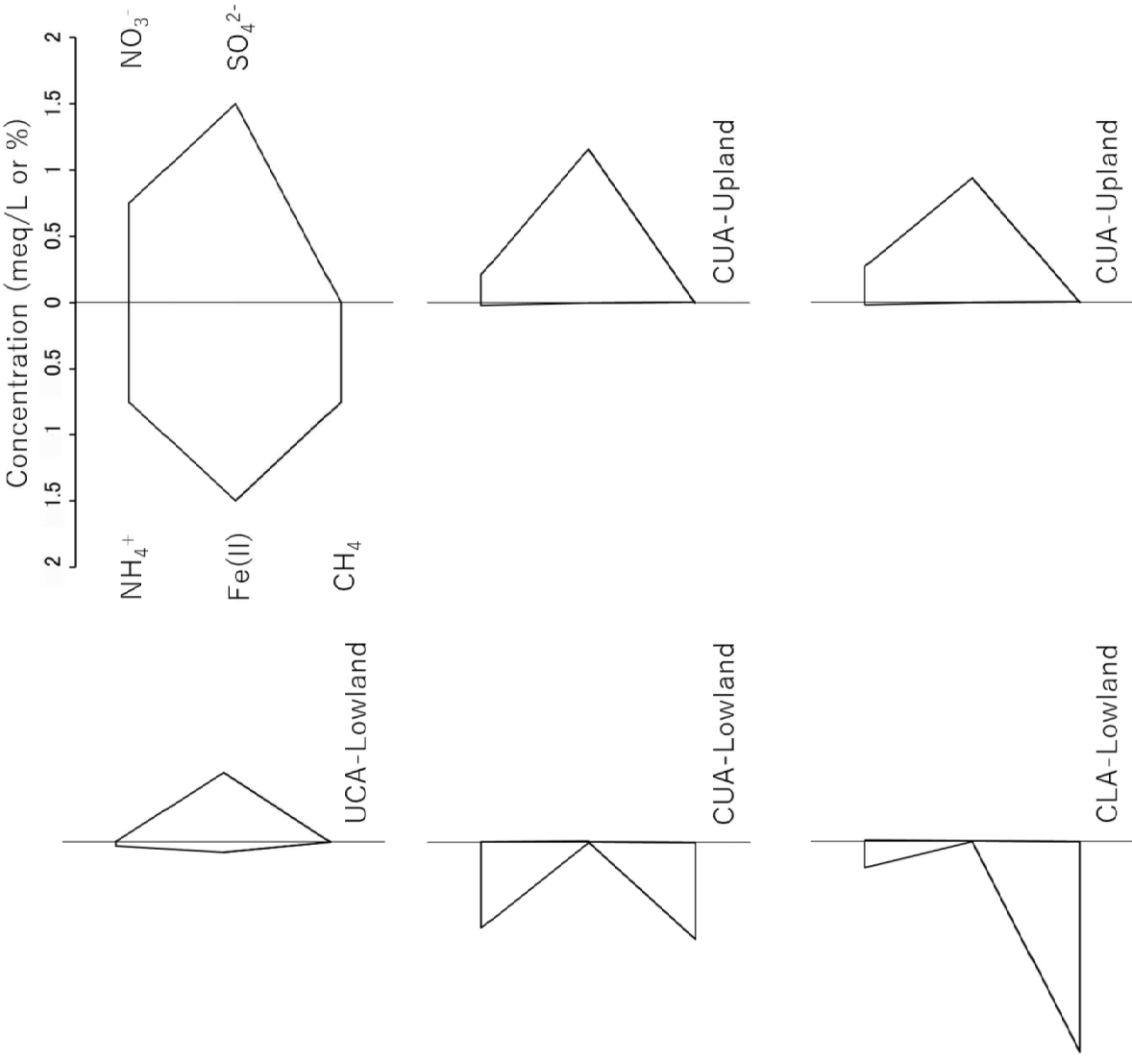


Fig. 8 A modified Stiff diagram for averaged concentration of groundwater redox sensitive chemical species (NO_3^- , NH_4^+ , and Fe(II) : meq/L and CH_4 : %) in the groundwater from three aquifers (UCA, CUA, and CLA) at the Lowland and Upland sites. UCA, CUA, and CLA stand for unconfined aquifer, confined upper aquifer, and confined lower aquifer, respectively.